

A Novel Haplotype with the R345W Mutation in the *EFEMP1* Gene Associated with Autosomal Dominant Drusen in a Japanese Family

Tomokazu Takeuchi,¹ Takaaki Hayashi,¹ Matthew Bedell,² Kang Zhang,² Hisashi Yamada,³ and Hiroshi Tsuneoka¹

PURPOSE. To describe ophthalmic and molecular genetic findings in a family of Japanese patients with Malattia leventinese (ML)/Doyle honeycomb retinal dystrophy (DHRD), also known as autosomal dominant drusen.

METHODS. Four patients with ML/DHRD, including a 42-year-old female proband, were ascertained. The proband underwent complete ophthalmic examinations, including fundus and electrodiagnostic investigations, and Humphrey visual field (VF) perimetry. Mutation screening of the *EFEMP1* gene and haplotype analysis were performed in the family, an Indian ML/DHRD family, and a branch of 1 of 39 ML/DHRD families in the United States, in which all affected patients shared a common haplotype.

RESULTS. A heterozygous missense mutation (p.R345W) was identified in all four Japanese patients and in affected patients of the other two families. This mutation was the only mutation that has been exclusively found in the gene. The disease haplotype in the Japanese family was different from those of the other two families. Clinically, central retinas were prominently affected in the proband and her mother, and subsequently the proband developed subfoveal choroidal neovascularization in the left eye, whereas her younger sister with the mutation, who was asymptomatic, exhibited only fine macular drusen. Long-term follow-up of Humphrey VF and multifocal-electroretinography (mfERG) in the proband also revealed progressive attenuation of macular function in the right eye.

CONCLUSIONS. This is the first report to describe a Japanese family with variable expressivity of ML/DHRD, in which a novel disease haplotype was identified. Humphrey VF and mfERG testing may be helpful in determining the long-term outcome of macular function. (*Invest Ophthalmol Vis Sci*. 2010;51:1643-1650) DOI:10.1167/iovs.09-4497

From the ¹Department of Ophthalmology and the ³Department of Molecular Genetics, Institute of DNA Medicine, The Jikei University School of Medicine, Tokyo, Japan; and the ²Institute for Genomic Medicine and Shiley Eye Center, University of California at San Diego, La Jolla, California.

Supported by grants from the Ministry of Education, Culture, Sports, Science and Technology of Japan [Grant-in-Aid for Scientific Research (C) 19592042] (TH); National Institutes of Health Grants R01EY14428 and R01EY14448; Foundation Fighting Blindness; the Macular Vision Research Foundation; and Research to Prevent Blindness (KZ).

Submitted for publication August 17, 2009; revised September 21, 2009; accepted September 22, 2009.

Disclosure: T. Takeuchi, None; T. Hayashi, None; M. Bedell, None; K. Zhang, None; H. Yamada, None; H. Tsuneoka, None

Corresponding author: Takaaki Hayashi, Department of Ophthalmology, The Jikei University School of Medicine, 3-25-8, Nishi-shimbashi, Minato-ku, Tokyo, 105-8461, Japan; taka@jikei.ac.jp.

Malattia leventinese (ML)¹/Doyle honeycomb retinal dystrophy (DHRD),² also known as autosomal dominant drusen (Mendelian Inheritance in Man [MIM] no. 126600), is a rare macular dystrophy characterized by the presence of innumerable drusen and alterations of the retinal pigment epithelium (RPE) in the posterior pole. Drusen are tiny yellow-white accumulations of extracellular material under the RPE on Bruch's membrane. Although drusen may appear in areas of the macula in early adult life, the presence of larger and more numerous drusen in the macula is a common early sign of age-related macular degeneration (AMD), the leading cause of central vision loss in developed countries. In the advanced stages of ML/DHRD, typically at age 40 to 50 years, central vision deteriorates and absolute scotomas develop as a result of extensive pigmentary changes, geographic atrophy, or choroidal neovascularization (CNV), either alone or in combination. Investigation of ML/DHRD may therefore provide important insight into the pathogenesis of AMD.

Linkage studies in families with ML/DHRD have mapped the disease locus to chromosome 2p16-21.³⁻⁷ In 1999, a single missense mutation (p.R345W) in the *EFEMP1* (known as *fibulin-3*, MIM *601548) gene was identified as responsible for ML/DHRD.⁸ In the original publication, all 39 families with the mutation were described as sharing a common haplotype with the p.R345W mutation.⁸ Since the initial report, the p.R345W mutation has been the sole mutation found in patients with ML/DHRD.⁹⁻¹³ Interestingly, Tartelin et al.¹⁰ reported two families (UK5 and UK6) with dominant drusen linked to the 2p16 locus that did not have an *EFEMP1* mutation. To our knowledge, however, no case of *EFEMP1*-associated ML/DHRD has been reported in the Japanese population.

This study was conducted to investigate whether the p.R345W mutation also can be a cause of ML/DHRD transmitted in an autosomal dominant manner in Japanese patients. Here we describe clinical and genetic findings of four patients with ML/DHRD (including the 42-year-old female proband) in a Japanese family, all whom had a novel haplotype with the p.R345W mutation.

PATIENTS AND METHODS

The protocol of this study was approved by the Institutional Research Board of The Jikei University School of Medicine. The protocol adhered to the tenets of the Declaration of Helsinki, and informed consent was obtained from all participants.

Clinical Studies

The study was conducted in a three-generation Japanese family (Family 1, JU 0136) with ML/DHRD. This family has been reported to be of Japanese ancestry by genealogy. Four patients (I-1, II-2, III-1, III-2) from Family 1 (Fig. 1A) underwent a standard ophthalmic examination,

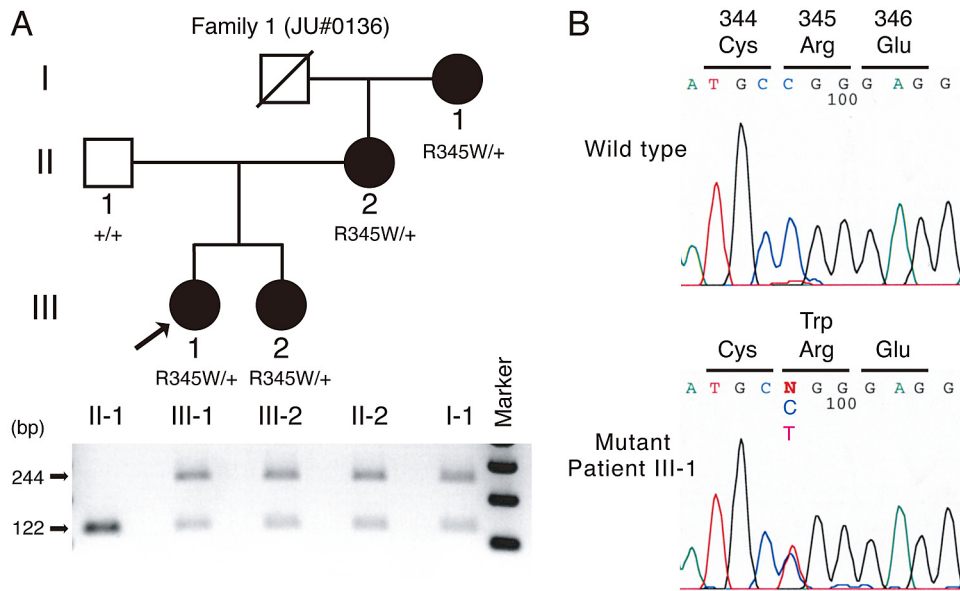


FIGURE 1. Pedigree of the Japanese family (Family 1, JU 0136) and polymerase chain reaction-restriction fragment length polymorphism (PCR-RFLP) analysis and sequencing results of the *EFEMP1* gene in Family 1. (A) Unaffected family members (males, *open squares*) and affected members (females, *solid circles*). *Arrow*: proband (III-1). *Slashed symbol*: deceased male. In PCR-RFLP analysis of available family members, the gel photograph demonstrates that the only wild-type allele from the unaffected father (II-1) is cut with *MspI*, resulting in two kinds of bands with 122 base pairs (bp). All affected family members (I-1, II-2, III-1, and III-2) are heterozygotes for the p.R345W mutation, showing an uncut band (244 bp) from the mutant allele and cut bands (122 bp). Marker, 100-bp ladder molecular weight marker. (B) Partial nucleotide sequencing of exon 10 in a subject with normal vision (wild type) and in the proband (III-1). A heterozygous variation (c.1033C>T) is shown that resulted in the substitution of Trp (TGG) for Arg (CGG) at amino acid position 345 (p.R345W).

sequences of exon 10 in a subject with normal vision (wild type) and in the proband (III-1). A heterozygous variation (c.1033C>T) is shown that resulted in the substitution of Trp (TGG) for Arg (CGG) at amino acid position 345 (p.R345W).

including decimal best-corrected visual acuity (BCVA), slit-lamp biomicroscopy, and dilated funduscopy. Additionally, the 42-year-old female proband (III-1) underwent fluorescein angiography (FA), indocyanine green angiography (ICGA) using a scanning laser ophthalmoscope (model 101; Rodenstock Instruments, Munich, Germany), fundus autofluorescence (FAF) imaging (F-10; Nidek Technologies, Aichi, Japan), and optical coherence tomography (OCT) (OCT3 Stratus; Carl Zeiss Meditec AG, Dublin, CA). Electro-oculography (EOG) and full-field electroretinography (ERG) were performed according to the protocols of the International Society for Clinical Electrophysiology of Vision. The procedure and conditions for ERG recording have been detailed elsewhere.^{14,15} EOG was recorded using a Ganzfeld stimulator and two red fixation lights at 15° left and right of center. Briefly, after pre-light adaptation, EOG potentials were recorded for 15 minutes in darkness followed by 15 minutes in the light phase with a background light of 100 photopic cd/m². The ratio of light peak to dark trough (Arden ratio) was determined. Mean Arden ratio of 11 control subjects (22 eyes) was 2.31 ± 0.33. Multifocal ERG (mfERG) was performed with maximally dilated pupils. Refractive errors were corrected. For stimulation, a black-and-white pattern of 61 hexagons was presented on a monitor at 200 cd/m² in the lit state and at 1 cd/m² in the dark state. Duration of data acquisition was 4 minutes, divided into 8 sessions of 30 seconds. Data analysis was performed with the VERIS science system (Electro Diagnostic Imaging Inc., San Mateo, CA). Visual fields (VF) were assessed using a Humphrey field analyzer (HFA; Carl Zeiss Meditec, Dublin, CA) with the central 30-2 Swedish Interactive Threshold Algorithm standard program. Mean deviation (MD) and pattern SD (PSD) lines were analyzed.

Mutation Analysis

Blood samples were obtained from five members in Family 1. DNA was extracted from peripheral blood leukocytes. Genomic DNA was isolated from peripheral white blood cells using a blood DNA isolation kit (Puregene; Gentra Systems, Minneapolis, MN) that was used as the template to amplify the *EFEMP1* gene. All primers were produced by Sigma Aldrich (Tokyo, Japan). All coding exons (exons 3–12) of the *EFEMP1* gene were amplified by polymerase chain reaction (PCR) using previously reported primers^{8,13} except for exons 5 and 8. We used primers *EFEMP1*-5cF (5'-CTGTCTCTGTCTGTGTATACC-3') and *EFEMP1*-5cR (5'-CTCACCACGAGGTGCACTTG-3') to amplify exon 5 (549 bp) and *EFEMP1*-8bF (5'-GTCAGCAGATGACGTAGGTAC-3') and *EFEMP1*-8bR (5'-ATCCCATGGGTAAGCGTTTG-3') to amplify exon 8

(338 bp). The PCR products were purified (QIAquick PCR Purification kit; Qiagen, Tokyo, Japan) and were used as the template for sequencing. Both strands were sequenced on an automated sequencer (3730xl DNA Analyzer; Applied Biosystems, Foster City, CA) using a terminator kit (BigDye, version 3.1; Applied Biosystems).

To screen a single nucleotide variation (c.1033C>T) found in the proband (III-1), PCR-restriction fragment length polymorphism (PCR-RFLP) analysis was performed. A 244-bp fragment of exon 10 was amplified by PCR using primers *EFEMP1*-10F (5'-CTTGCAAACA-GAATCTGCCA-3') and *EFEMP1*-10R (5'-TCCTCACTTTCAAAAGTTCT-GATTT-3'). The PCR products were digested with a restriction endonuclease, *MspI* (New England Biolabs, Beverly, MA). The only wild-type allele was cleaved with the enzyme, resulting in two 122-bp fragments.

Haplotype Analysis

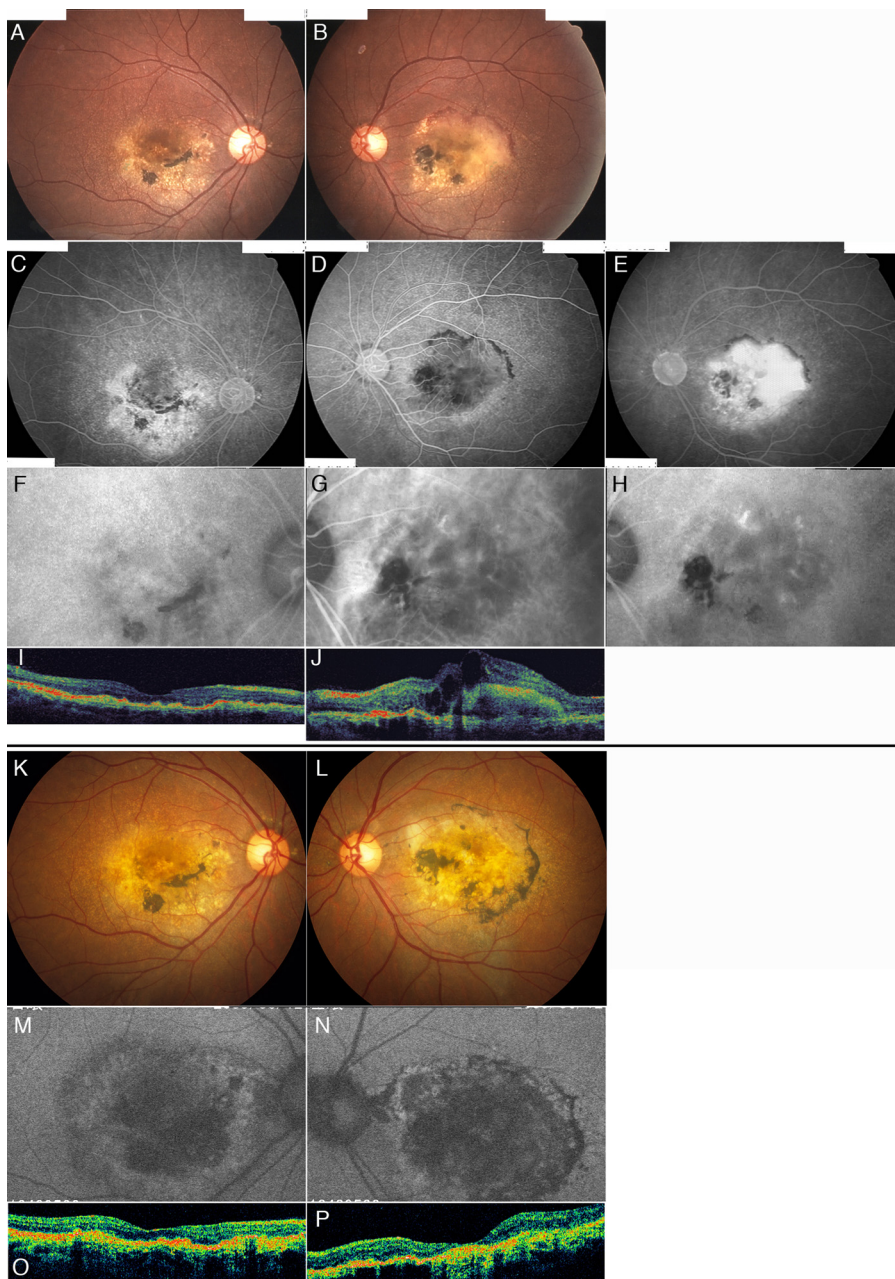
To test whether the mutation haplotype of the Japanese family (Family 1) was identical with that in the original 1999 report,⁸ two additional families (Family 2 and Family 3) with the clinical phenotype of DHRD/ML were examined. Family 2 and Family 3 corresponded to the previously reported Family A and Family B, respectively.¹⁶ Family 2 is a branch of one of the families described in the original report in 1999,⁸ and Family 3 is from India.¹⁶ The haplotype of Family 1 was compared with those of Family 2 and Family 3, who had been previously identified,¹⁶ using two microsatellite markers (D2S378 and D2S2352), six polymorphic intragenic single nucleotide polymorphisms (SNPs) (rs1430197, rs1430193, rs3791675, rs3791676, rs1346786, and rs3791679), and two polymorphic SNPs (rs1346789 and rs4352264) in the vicinity of the 5'-end of the *EFEMP1* gene. These markers and SNPs were located in the order of pter (short-arm telomeric end)—D2S2352- rs4352264- rs1346789- rs3791679- rs1346786- rs3791676- rs3791675- rs1430193- rs1430197- D2S378-cen (centromere). The interval between D2S378 and D2S2352 was estimated to be approximately 3.4 Mbp. For analysis of microsatellite markers, PCR amplification was performed using primers with different fluorophores (one was 5'-end FAM-labeled and the other was 5'-end HEX-labeled), followed by analysis with a DNA analyzer (3130xl Genetic Analyzer; Applied Biosystems) and software (GeneMapper; Applied Biosystems).

RESULTS

Clinical Findings

Patient III-1. The proband, a 42-year-old Japanese woman with no history of smoking, was referred for retinal evaluation

FIGURE 2. Photographs and images of the proband (III-1) at age 43 (A–J). Fundus photographs of the right (A) and left (B) eyes showing innumerable basal laminar drusen in a radial distribution, peripapillary drusen, large yellowish dense drusen, and hyperplasia of the retinal pigment epithelium (RPE) in both eyes. An exudative lesion surrounded by a thin rim of sub-retinal hemorrhage is seen in the left eye (B). Late-phase fluorescein angiogram (FA) showing numerous hyperfluorescent dots corresponding to basal laminar drusen, hyperfluorescent lesions of confluent drusen, and blocked fluorescence by RPE hyperplasia in the right eye (C). FA of the left eye showing large, well-defined choroidal neovascularization (CNV) surrounded by a thin rim of blocked fluorescence in the early phase (D) and prominent fluorescein leakage secondary to predominantly classic CNV in the late phase (E). Indocyanine green angiography showing no CNV in the right eye (F), distinct CNV of the early (G) and late phases (H) in the left eye. Horizontal optical coherence tomography (OCT) images showing normal foveal thickness and irregular hyperreflective lesions on the RPE-Bruch's membrane complex in the right eye (I) and macular thickening with cystoid macular edema and the elevated RPE-Bruch's membrane band in the left eye (J). Photographs and images of the proband (III-1) at age 48 (K–P). Fundus photograph of the right (K) and left (L) eyes showing that the yellowish dense drusen were more confluent and the lesions of pigmentation were more prominent. Fundus autofluorescence (FAF) image of the right (M) and left (N) eyes showing generalized reduction of macular FAF, with areas of increased FAF corresponding to the confluent drusen. Horizontal OCT images showing preservation of the retinal thickness in the right eye (O) and macular atrophy in the left eye (P).



of distorted vision in the left eye. After evaluation for 1.5 years by another ophthalmologist who diagnosed bilateral macular degeneration, she noticed progressive distortion of vision and severe vision loss in the left eye (decimal BCVA decreased from 1.2 to 0.08 in the left eye and remained constant at 1.5 in the right). She was then examined by one of the authors. Funduscopic examination showed basal laminar drusen and hyperplasia of the RPE in the macular areas in both eyes (Figs. 2A, B) with hyperfluorescent dots corresponding to basal laminar drusen and blocked fluorescence by RPE hyperplasia in both eyes (Figs. 2C, D). Further, a large choroidal neovascular membrane with characteristics of a predominantly classic lesion was seen in the subfoveal region of the left eye (Figs. 2D, E). Late-phase ICGA showed no CNV in the right eye (Fig. 2F), whereas distinct choroidal neovascular membranes were seen in the early (Fig. 2G) and late (Fig. 2H) phases in the left eye. Horizontal OCT (6-mm line scan) images showed normal foveal thickness and irregular hyperreflective lesions on the RPE-

Bruch's membrane complex (saw-toothed pattern) corresponding to the large macular drusen in the right eye (Fig. 2I), whereas thickening of the left macula with cystoid macular edema and the elevated RPE-Bruch's membrane band was caused by Gass type-2 CNV (Fig. 2J). No treatment was administered because photodynamic therapy (PDT) with verteporfin and antivascular endothelial growth factor (anti-VEGF) therapies were not available at that time. She has monitored for nearly 6 years (since age 42).

At age 48, BCVA was 1.5 (right eye) and 0.1 (left eye), the yellowish dense drusen were more confluent, and the pigmentation lesions were more prominent in both maculae (Figs. 2K, L) compared with the fundus findings at age 43 (Figs. 2A, B). The FAF images showed a generalized reduction in macular FAF, with areas of increased FAF corresponding to the confluent drusen in both eyes (Figs. 2M, N). Horizontal OCT (6-mm line scan) images showed the preservation of retinal thickness in the right eye (Fig. 2O) and macular atrophy in the left eye (Fig. 2P).

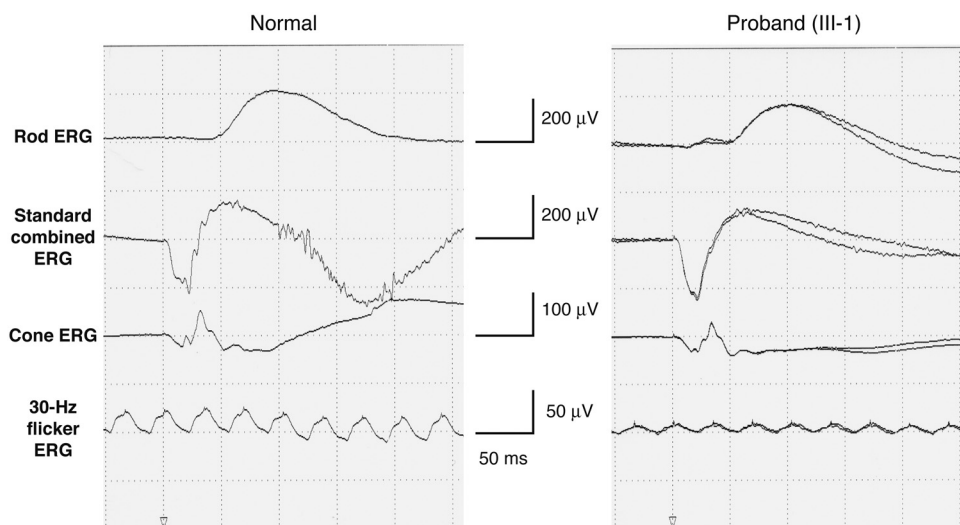


FIGURE 3. Full-field electroretinograms of a subject with normal vision and the proband (III-1) showing normal rod b-wave responses, normal standard combined (mixed rod-plus-cone) responses, the lowest limit of normal cone responses, and reduced 30-Hz flicker responses in the proband. ms, milliseconds; μ V, microvolts.

Full-field ERG and EOG were performed when she was 42 years old. The ERG showed normal rod b-wave responses, normal standard combined (mixed rod-plus-cone) responses, the lowest limit of normal cone responses, and reduced 30-Hz flicker responses in both eyes (Fig. 3). Arden ratios of EOG were 2.16 in the right eye and 2.03 in the left, both within the normal range.

In mfERG, the central peak and paracentral responses were bilaterally attenuated (Fig. 4A) at age 42. Four years later, the paracentral responses were more attenuated (Fig. 4B) than those at age 42 in the right eye, whereas the whole responses were much more severely attenuated (Fig. 4B) than those at age 42 in the left, in which CNV (Fig. 2J) and subsequent macular atrophy (Fig. 2P) developed.

Nine HFA VF tests were examined over a follow-up period of nearly 6 years. The MD slope was stable in the right eye but was considerably negative in the left eye, in which CNV developed (Fig. 5A). The PSD slope of the left eye was worse than that of the right eye (Fig. 5B).

Patient II-2. Patient II-2 was a 68-year-old woman, the mother of the proband, who had never had blurred or distorted vision. Her decimal BCVA was 1.0 in the right eye and 0.8 in the left. She had innumerable drusen in a radial distribution, large yellowish confluent drusen, RPE alterations, and peripapillary drusen (Figs. 6A, B) but no exudative lesions. The fundus findings were similar to those of patient III-1.

Patient III-2. Patient III-2 was a 40-year-old woman, the sister (2 years younger) of the proband, who had never had any ocular symptoms such as blurred or distorted vision. Her decimal BCVA was 1.2 in both eyes. Color fundus photographs showed innumerable, small, discrete drusen in a radial pattern and peripapillary drusen in the posterior poles of both eyes (Figs. 6C, D).

Molecular Genetic Findings

Mutation analysis of the *EFEMP1* gene revealed a heterozygous variant (c.1033C>T in exon 10) in the proband (III-1). This variant resulted in the substitution of tryptophan (TGG) for arginine (CGG) at amino acid position 345 (Fig. 1B). The missense mutation (p.R345W) was identical with the sole mutation previously reported in the *EFEMP1* gene. No other nucleotide variations of this gene were detected in the proband. To screen the mutation, PCR restriction fragment length polymorphism analysis was performed in the other family members (I-1, II-1, II-2, III-2) whose DNA samples were available. Agarose-gel analysis showed that the 244-bp PCR prod-

ucts from wild-type alleles (arginine 345/arginine 345, II-1) were cut with the restriction enzyme *MspI*, resulting in two 122-bp bands, whereas all the patients (I-1, II-2, III-1, III-2) with diagnoses of ML/DHRD carried both wild-type (arginine 345) and mutant (tryptophan 345) alleles (Fig. 1A), consistent with autosomal dominant transmission. The mutation was not found in 100 Japanese and 500 Caucasian subjects without any retinal diseases.

Disease haplotypes with the p.R345W mutation were determined in all three families and revealed that Family 1 exhibited a distinctive disease haplotype (8-T-G-C-M-T-G-A-T-G-3) (Fig. 7). In addition, we confirmed that the haplotype of Family 2 (1-C-A-T-M-C-A-G-A-G-1), which was identical with the previously reported haplotype,^{8,16} was different from the haplotype (6-T-A-T-M-T-G-A-T-A-6) of Family 3 from India (Fig. 7). Thus, not only two microsatellite markers but also intragenic SNPs differed among the three families. Consequently, the distinctive haplotype with the p.R345W mutation in Family 1 indicated that the p.R345W mutation arose independently within the Japanese ancestry of the family.

DISCUSSION

We describe three generations of a Japanese family (Family 1) that has four patients with ML/DHRD with the heterozygous *EFEMP1* mutation (p.R345W), the only mutation exclusively found in patients with ML/DHRD. A major finding of the molecular genetic study was that the disease haplotype in Family 1 has not been reported to date. In the original publication describing the p.R345W mutation, all 39 families were reported to have it.⁸ The absence of de novo p.R345W mutations in the 39 families, and complete sharing of alleles of intragenic *EFEMP1* SNPs among them,⁸ suggested that the mutation occurred only once, in a common ancestor of every affected patient. Thus, the 39 families shared a common haplotype that was identical with the haplotype of Family 2 (Family A in the source publication¹⁶). Family 3 (Family B in the source publication¹⁶), which was from India, had a unique haplotype with the mutation.¹⁶ When comparing these haplotypes, that of Family 1 was distinctly different from those of Family 2 and Family 3 (Fig. 7), suggesting that the mutation in Family 1 might have occurred independently in a common Japanese ancestor or founder. Thus, although the three disease haplotypes were distinctive among ethnic groups, the phenotype resulting from the mutation was a uniform macular dystrophy, ML/DHRD. This excluded the possibility that the amino

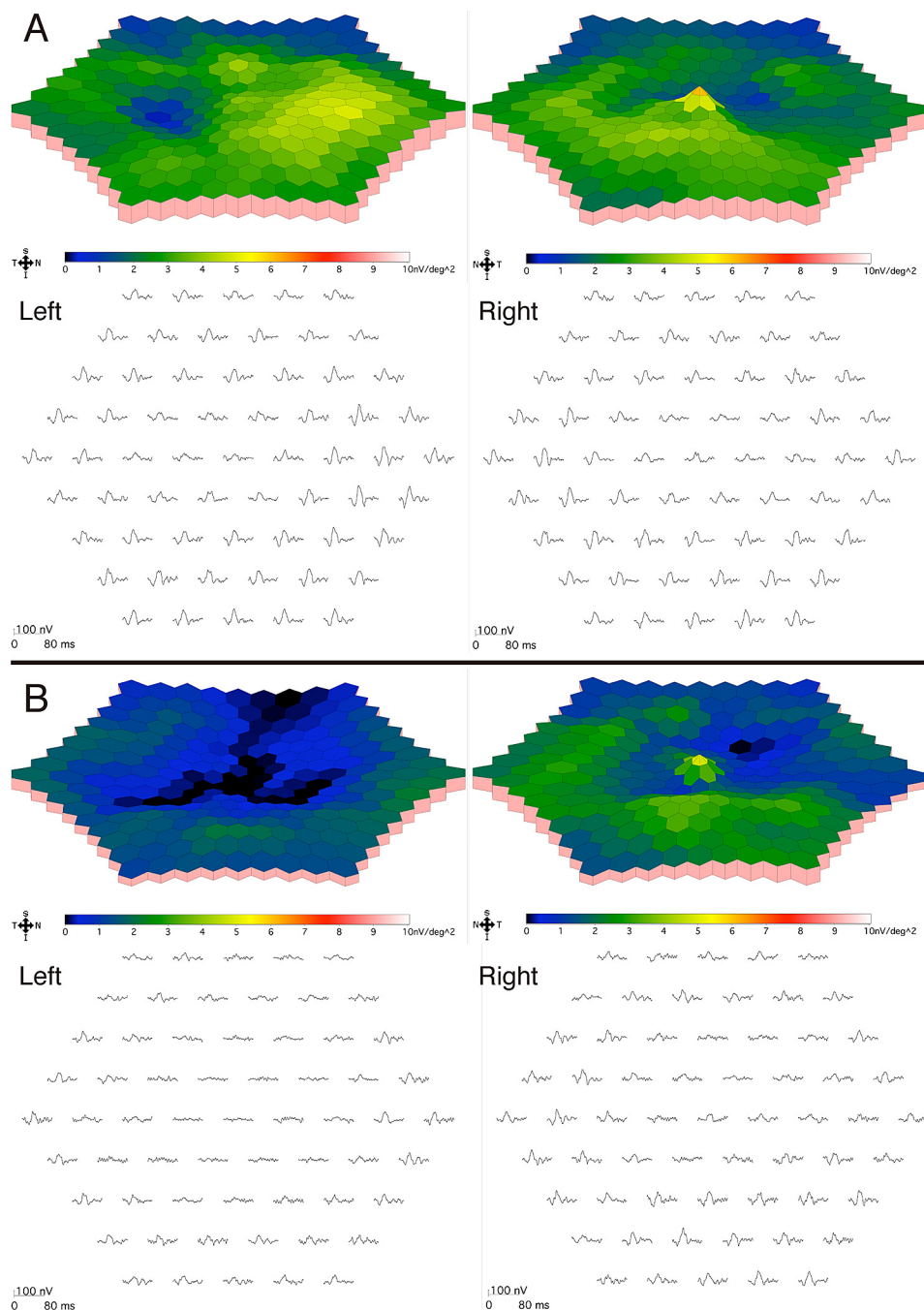


FIGURE 4. Multifocal electroretinograms of the proband (III-1). At age 42 (A), the central peak and paracentral responses were bilaterally attenuated. At age 46 (B), the paracentral responses in the right eye were more attenuated, whereas the whole responses throughout the left eye were much more severely attenuated than those at age 42.

acid substitution variant (p.R345W) was in linkage disequilibrium with a true disease-causing mutation located in the vicinity of the *EFEMP1* gene, in turn confirming that ML/DHRD is indeed caused by the p.R345W mutation.

Variability of disease expression is seen in many autosomal dominant disorders and is generally ascribed to the modifying effects of other genetic attributes, environmental factors, or both. Phenotypic studies have demonstrated that ML/DHRD with the p.R345W mutation manifests intrafamilial phenotypic variability.^{5,13,17} This variability of disease severity was also observed in Family 1. Patient III-2, who was asymptomatic, exhibited only fine macular radial and peripapillary drusen (Figs. 6C, D), whereas her sister, who was 2 years older (the proband, patient III-1), was severely affected in the central retina, in which densely confluent drusen and extensive pigmentary alterations were seen (Fig. 2), similar to the fundus

findings of their mother (II-2; Figs. 6A, B). Patient III-1 subsequently developed subfoveal CNV in the left eye at age 43 (Fig. 2), which resulted in severe vision loss and deterioration of HFA MD slopes (Fig. 5). It is generally understood that drusen formation, rather than CNV, is the typical finding associated with ML/DHRD. In fact, it was reported that CNV may be an infrequent complication of ML/DHRD based on the finding that only 1 of 24 patients with ML/DHRD exhibited CNV.¹³ However, other clinical studies have described CNV and subretinal hemorrhage in patients with ML/DHRD.^{18–20} Accordingly, ophthalmologists should be aware of the potential risk for the most serious and sight-threatening complication in patients with ML/DHRD, namely CNV.

A biochemical and histologic study using donor eyes demonstrated that mutant EFEMP1 carrying the p.R345W mutation is misfolded and secreted inefficiently.²¹ The misfolded

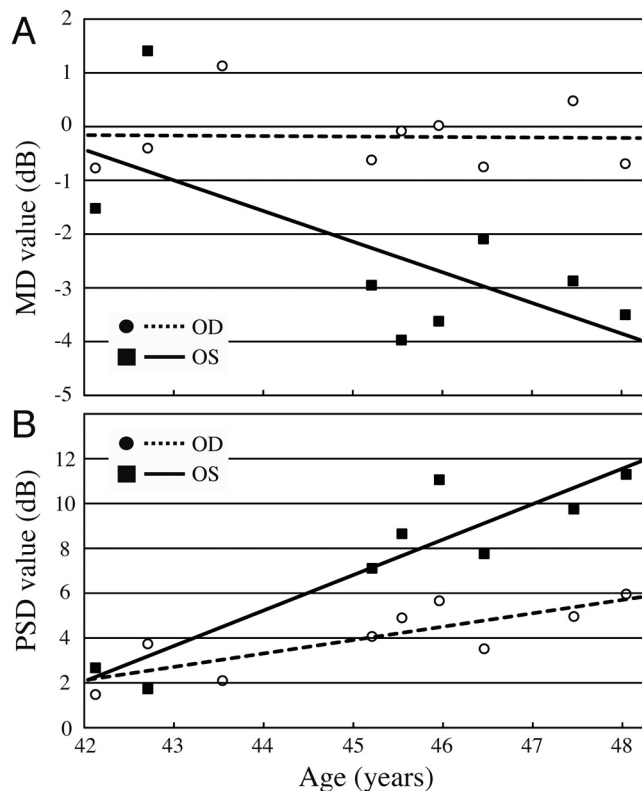


FIGURE 5. Results of nine visual field tests using a Humphrey field analyzer showing (A) mean deviation (MD) and (B) pattern SD (PSD) values (decibels, dB) during nearly 6 years of follow-up.

EFEMP1 protein accumulates within the RPE, and it is the aberrant accumulation of EFEMP1 that underlies drusen formation in ML/DHRD.²¹ Similar histopathologic findings were also observed in knock-in mice carrying the heterozygous and homozygous p.R345W mutations.^{16,22} In a human RPE cell line, the accumulation of mutant EFEMP1 led to the upregulation of VEGF expression.²³ Levels of VEGF were also significantly increased in the vitreous of patients with CNV, suggesting that VEGF may be involved in subretinal angiogenesis.²⁴ Furthermore, the formation of CNV was associated with increased VEGF expression in animal models.^{25,26} Given that hypoxia is a major stimulator of VEGF in RPE cells,²⁷ we speculate that the dense confluence of drusen caused by mutant EFEMP1 might lead to focal hypoxia by blocking the diffusion of oxygen from the choriocapillaris to the RPE, resulting in the increased expression of VEGF and the consequent development of CNV. Although the mechanism underlying CNV in ML/DHRD remains elusive, the pathogenesis of CNV development in ML/DHRD may be similar to that of neovascular AMD, in which VEGF plays a pivotal role in promoting CNV. Treatments effective against CNV and neovascular AMD are now available, namely PDT with verteporfin^{28,29} and anti-VEGF therapies.³⁰⁻³³ The efficacy of PDT with verteporfin in closure of the neovascular membranes in one patient with ML/DHRD has been reported.²⁰ These treatments may, therefore, be options if the decreased visual acuity in the right eye of patient III-1 is subsequently found to be caused by CNV.

Consistent with previous OCT findings in ML/DHRD,³⁴⁻³⁶ OCT in the right eye (Figs. 2I, O) showed a saw-toothed pattern in the RPE-Bruch's membrane complex corresponding to macular drusen. Electrophysiological findings (Fig. 3) agreed with those of previously reported cases, in which the EOG Arden ratios, scotopic rod, and mixed rod-plus-cone responses were within the normal range^{37,38} and the 30-Hz flicker responses were diminished.¹⁷ To our knowledge, no long-term follow-up

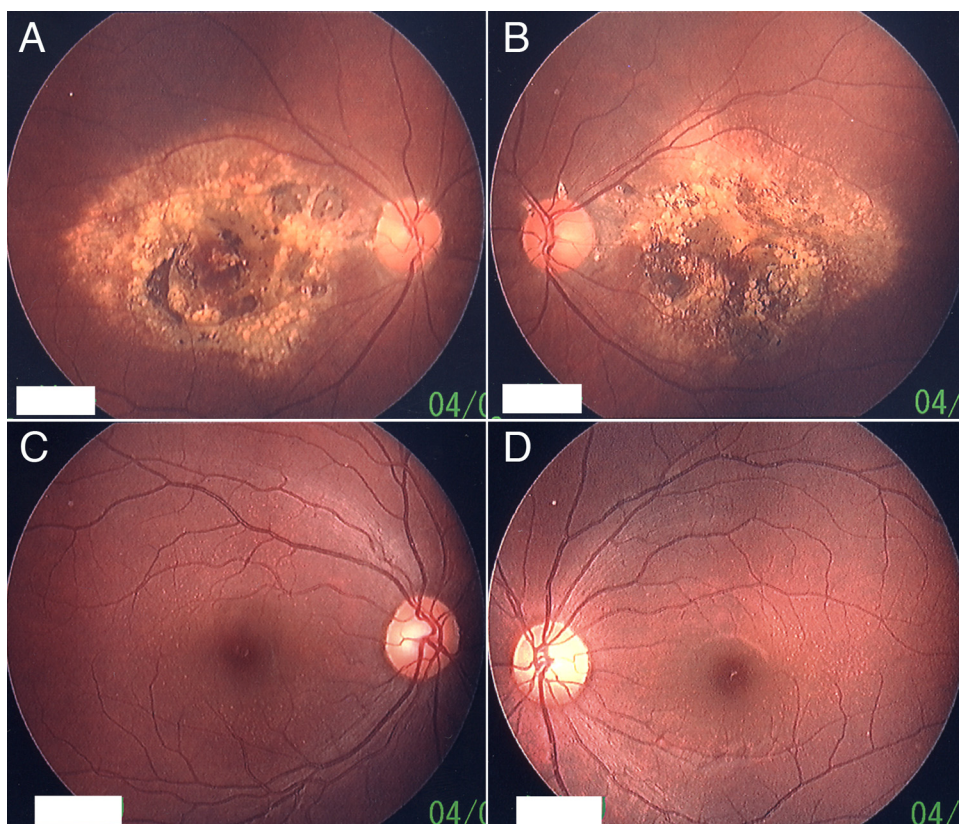


FIGURE 6. Fundus photograph on the right (A) and left (B) eyes of patient II-2 at age 68 showing fundus findings similar to those of the proband (Fig. 2), except for the development of choroidal neovascularization. Fundus photograph on the right (C) and left (D) eyes of patient III-2 at age 40 showing numerous small and discrete drusen in the posterior poles.

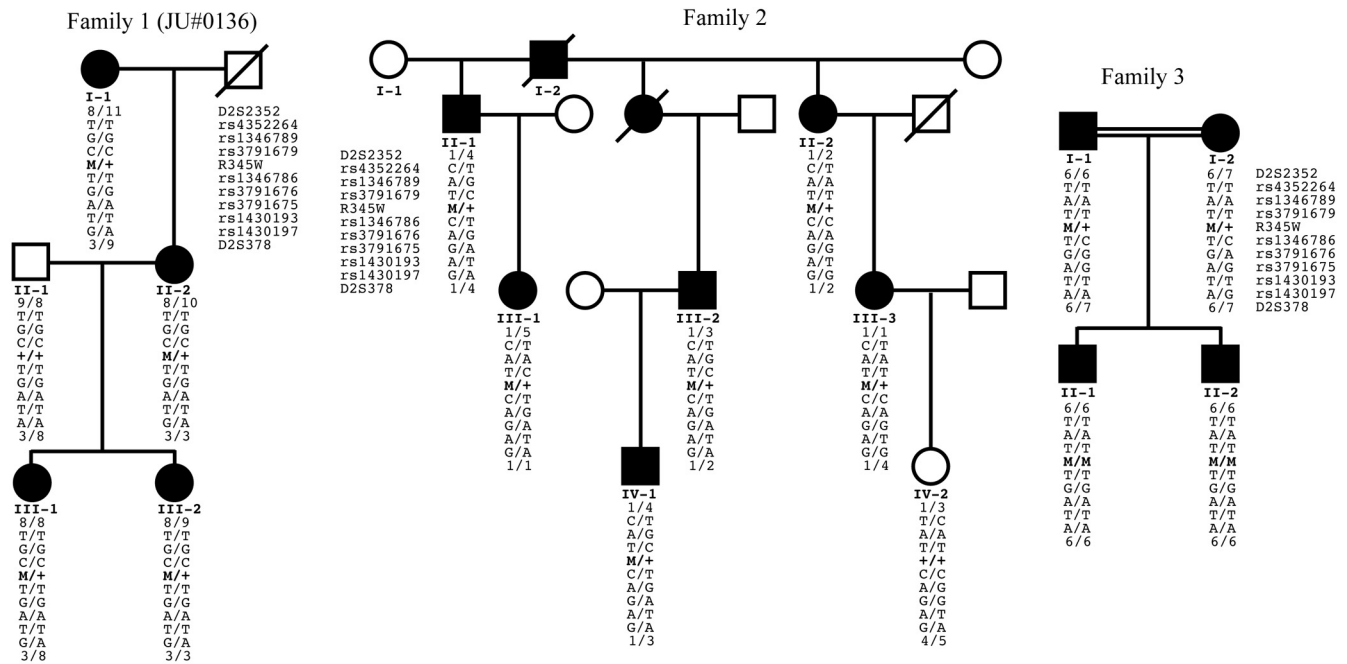


FIGURE 7. Pedigrees of three Malattia leventinese ML/DHRD families with the p.R345W mutation in the *EFEMP1* gene. *Left:* pedigree of the Japanese family (Family 1, JU 0136) with the novel haplotype. *Middle:* pedigree of Family 2 corresponding to Family A,¹⁶ a branch of one of the 39 US ML/DHRD families in which all affected patients shared a common haplotype.⁸ *Right:* pedigree of Family 3, from India, corresponding to the previously described Family B.¹⁶ Haplotype data for two microsatellite markers flanking the *EFEMP1* gene and eight SNPs within the *EFEMP1* gene are shown in five members of Family A, seven of Family B, and four of Family C. Family 1 exhibits a distinctive disease haplotype (8-T-G-C-M-T-G-A-T-G-3). Disease haplotype of Family 2 was 1-C-A-T-M-C-A-G-A-G-1, and that of Family 3 was 6-T-A-T-M-T-G-A-T-A-6. Family members are identified by generation and individual numbers. *Squares*, males; *circles*, females; *slashed symbols*, deceased; *solid symbols*, affected; *open symbols*, unaffected; +, wild-type; M, the p.R345W mutation.

of macular function in *EFEMP1*-associated ML/DHRD has been reported to date. Regarding macular function of the right eye, good visual acuity and HFA MD values have been sustained during 6 years of follow-up (Fig. 5A). However, not only have HFA PSD values deteriorated over the follow-up period (Fig. 5B), mfERG responses have been progressively attenuated for 4 years (Fig. 4). These results indicate gradual disease progression in the right eye, similar to the way in which nonexudative AMD progresses to geographic atrophy, a form of advanced atrophic AMD. Long-term follow-up of HFA and mfERG to assess the possible progressive attenuation of macular function would, therefore, be beneficial.

In summary, this is the report of a Japanese family with variable expressivity of *EFEMP1*-associated ML/DHRD in which a novel disease haplotype was identified. Before the development of CNV, periodic mfERG and HFA testing may be useful in assessing whether macular function is progressively attenuated. When CNV develops during follow-up in ML/DHRD, treatments aimed at neovascular AMD should be considered given that the mechanisms of CNV development in the two diseases may be similar.

References

- Vogt A. Die Ophthalmoskopie im Rotfreien Licht. In: Graefe A, Saemisch T, eds. *Handbuch der gesamten Augenheilkunde: Untersuchungsmethoden*. 3rd ed. Berlin: Leipzig, Verlag von Wilhelm Engelmann; 1925:1-118.
- Doyme RW. A peculiar condition of choroiditis occurring in several members of the same family. *Trans Ophthalmol Soc UK*. 1899;19:71.
- Gregory CY, Evans K, Wijesuriya SD, et al. The gene responsible for autosomal dominant Doyme's honeycomb retinal dystrophy (DHRD) maps to chromosome 2p16. *Hum Mol Genet*. 1996;5:1055-1059.
- Héon E, Piguet B, Munier F, et al. Linkage of autosomal dominant radial drusen (malattia leventinese) to chromosome 2p16-21. *Arch Ophthalmol*. 1996;114:193-198.
- Edwards AO, Klein ML, Berselli CB, et al. Malattia leventinese: refinement of the genetic locus and phenotypic variability in autosomal dominant macular drusen. *Am J Ophthalmol*. 1998;126:417-424.
- Kermani S, Gregory-Evans K, Tarttelin EE, et al. Refined genetic and physical positioning of the gene for Doyme honeycomb retinal dystrophy (DHRD). *Hum Genet*. 1999;104:77-82.
- Taymans SE, Kirschner LS, Giatzakis C, Stratakis CA. Radiation hybrid mapping of chromosomal region 2p15-p16: integration of expressed and polymorphic sequences maps at the Carney complex (CNC) and Doyme honeycomb retinal dystrophy (DHRD) loci. *Genomics*. 1999;56:344-349.
- Stone EM, Lotery AJ, Munier FL, et al. A single *EFEMP1* mutation associated with both malattia leventinese and Doyme honeycomb retinal dystrophy. *Nat Genet*. 1999;22:199-202.
- Matsumoto M, Traboulsi EL. Dominant radial drusen and Arg345Trp *EFEMP1* mutation. *Am J Ophthalmol*. 2001;131:810-812.
- Tarttelin EE, Gregory-Evans CY, Bird AC, et al. Molecular genetic heterogeneity in autosomal dominant drusen. *J Med Genet*. 2001;38:381-384.
- Guymer RH, McNeil R, Cain M, et al. Analysis of the Arg345Trp disease-associated allele of the *EFEMP1* gene in individuals with early onset drusen or familial age-related macular degeneration. *Clin Exp Ophthalmol*. 2002;30:419-423.
- Narendran N, Guymer RH, Cain M, Baird PN. Analysis of the *EFEMP1* gene in individuals and families with early onset drusen. *Eye*. 2005;19:11-15.
- Michaelides M, Jenkins SA, Brantley MA Jr, et al. Maculopathy due to the R345W substitution in fibulin-3: distinct clinical features, disease variability, and extent of retinal dysfunction. *Invest Ophthalmol Vis Sci*. 2006;47:3085-3097.

14. Hayashi T, Gekka T, Goto-Omoto S, et al. Novel NR2E3 mutations (R104Q, R334G) associated with a mild form of enhanced S-cone syndrome demonstrate compound heterozygosity. *Ophthalmology*. 2005;112:2115-2122.
15. Hayashi T, Gekka T, Takeuchi T, Goto-Omoto S, Kitahara K. A novel homozygous GRK1 mutation (P391H) in 2 siblings with Oguchi disease with markedly reduced cone responses. *Ophthalmology*. 2007;114:134-141.
16. Fu L, Garland D, Yang Z, et al. The R345W mutation in EFEMP1 is pathogenic and causes AMD-like deposits in mice. *Hum Mol Genet*. 2007;16:2411-2422.
17. Evans K, Gregory CY, Wijesuriya SD, et al. Assessment of the phenotypic range seen in Doyme honeycomb retinal dystrophy. *Arch Ophthalmol*. 1997;115:904-910.
18. Zech JC, Zaouche S, Mourier F, et al. Macular dystrophy of malattia leventinese: a 25-year follow-up. *Br J Ophthalmol*. 1999;83:1195-1196.
19. Pager CK, Sarin LK, Federman JL, et al. Malattia leventinese presenting with subretinal neovascular membrane and hemorrhage. *Am J Ophthalmol*. 2001;131:517-518.
20. Dantas MA, Slakter JS, Negrão S, et al. Photodynamic therapy with verteporfin in malattia leventinese. *Ophthalmology*. 2002;109:296-301.
21. Marmorstein LY, Munier FL, Arsenijevic Y, et al. Aberrant accumulation of EFEMP1 underlies drusen formation in malattia leventinese and age-related macular degeneration. *Proc Natl Acad Sci U S A*. 2002;99:13067-13072.
22. Marmorstein LY, McLaughlin PJ, Peachey NS, Sasaki T, Marmorstein AD. Formation and progression of sub-retinal pigment epithelium deposits in Efemp1 mutation knock-in mice: a model for the early pathogenic course of macular degeneration. *Hum Mol Genet*. 2007;16:2423-2432.
23. Roybal CN, Marmorstein LY, Vander Jagt DL, Abcouwer SF. Aberrant accumulation of fibulin-3 in the endoplasmic reticulum leads to activation of the unfolded protein response and VEGF expression. *Invest Ophthalmol Vis Sci*. 2005;46:3973-3979.
24. Wells JA, Murthy R, Chibber R, et al. Levels of vascular endothelial growth factor are elevated in the vitreous of patients with subretinal neovascularisation. *Br J Ophthalmol*. 1996;80:363-366.
25. Ishibashi T, Hata Y, Yoshikawa H, et al. Expression of vascular endothelial growth factor in experimental choroidal neovascularization. *Graefes Arch Clin Exp Ophthalmol*. 1997;35:159-167.
26. Shen WY, Yu MJ, Barry CJ, Constable IJ, Rakoczy PE. Expression of cell adhesion molecules and vascular endothelial growth factor in experimental choroidal neovascularisation in the rat. *Br J Ophthalmol*. 1998;82:1063-1071.
27. Mousa SA, Lorelli W, Campochiaro PA. Role of hypoxia and extracellular matrix-integrin binding in the modulation of angiogenic growth factors secretion by retinal pigmented epithelial cells. *J Cell Biochem*. 1999;74:135-143.
28. Photodynamic therapy of subfoveal choroidal neovascularization in age-related macular degeneration with verteporfin: one-year results of 2 randomized clinical trials-TAP report. Treatment of age-related macular degeneration with photodynamic therapy (TAP) Study Group. *Arch Ophthalmol*. 1999;117:1329-1345.
29. Verteporfin therapy of subfoveal choroidal neovascularization in age-related macular degeneration: two-year results of a randomized clinical trial including lesions with occult with no classic choroidal neovascularization-verteporfin in photodynamic therapy report 2. *Am J Ophthalmol*. 2001;131:541-560.
30. Gragoudas ES, Adamis AP, Cunningham ET Jr, Feinsod M, Guyer DR. Pegaptanib for neovascular age-related macular degeneration. *N Engl J Med*. 2004;351:2805-2816.
31. Rosenfeld PJ, Moshfeghi AA, Puliafito CA. Optical coherence tomography findings after an intravitreal injection of bevacizumab (avastin) for neovascular age-related macular degeneration. *Ophthalmic Surg Lasers Imaging*. 2005;36:331-335.
32. Rosenfeld PJ, Brown DM, Heier JS, et al. Ranibizumab for neovascular age-related macular degeneration. *N Engl J Med*. 2006;355:1419-1431.
33. Brown DM, Kaiser PK, Michels M, et al. Ranibizumab versus verteporfin for neovascular age-related macular degeneration. *N Engl J Med*. 2006;355:1432-1444.
34. Gaillard MC, Wolfensberger TJ, Uffer S, et al. [Optical coherence tomography in malattia leventinese]. *Klin Monatsbl Augenheilkd*. 2005;222:180-185.
35. Souied EH, Leveziel N, Letien V, et al. Optical coherent tomography features of malattia leventinese. *Am J Ophthalmol*. 2006;141:404-407.
36. Gerth C, Zawadzki RJ, Werner JS, Heon E. Retinal microstructure in patients with EFEMP1 retinal dystrophy evaluated by Fourier domain OCT. *Eye*. 2009;23:480-483.
37. Fishman GA, Carrasco C, Fishman M. The electro-oculogram in diffuse (familial) drusen. *Arch Ophthalmol*. 1976;94:231-233.
38. Haimovici R, Wroblewski J, Piguet B, et al. Symptomatic abnormalities of dark adaptation in patients with EFEMP1 retinal dystrophy (malattia leventinese/Doyme honeycomb retinal dystrophy). *Eye*. 2002;16:7-15.